Delft University of Technology

Tube-wave Generation Due to Permeable Layers in a VSP Experiment
A New Model Elucidating the Effect of Dip Angles

Minato, Shohei; Ghose, Ranajit

DOI
10.3997/2214-4609.201701198

Publication date
2017

Document Version
Accepted author manuscript

Published in
79th EAGE Conference & Exhibition 2017

Citation (APA)
Minato, S., & Ghose, R. (2017). Tube-wave Generation Due to Permeable Layers in a VSP Experiment: A New Model Elucidating the Effect of Dip Angles. In *79th EAGE Conference & Exhibition 2017: Paris, France* Article We A5 11 EAGE. https://doi.org/10.3997/2214-4609.201701198

Important note
To cite this publication, please use the final published version (if applicable).
Please check the document version above.

Copyright
Other than for strictly personal use, it is not permitted to download, forward or distribute the text or part of it, without the consent of the author(s) and/or copyright holder(s), unless the work is under an open content license such as Creative Commons.

Takedown policy
Please contact us and provide details if you believe this document breaches copyrights.
We will remove access to the work immediately and investigate your claim.

This work is downloaded from Delft University of Technology.
For technical reasons the number of authors shown on this cover page is limited to a maximum of 10.

This is an Accepted Manuscript of a paper published by EAGE
https://doi.org/10.3997/2214-4609.201701198

Tube-wave generation due to permeable layers in a VSP experiment: a new model elucidating the effect of dip angles

Shohei Minato and Ranajit Ghose

Abstract

The hydraulic properties of subsurface fractures are critically important in the exploration of geothermal and hydrocarbon reservoirs. The analysis of tube waves (low-frequency Stoneley waves propagating along a fluid-filled borehole) is a promising approach to estimate the hydraulic properties of fractures intersecting a borehole. We present a new model for tube-wave generation in a borehole (VSP) by a permeable structure characterized by certain values of porosity and permeability. Contrary to the conventional theory, the new model accounts for the layer stiffness in the deformation process and it is valid for the large tube-wave amplitude. For the first time, it was possible to show a clear connection between the permeable-layer model and the parallel-wall open fracture model developed earlier. The generated tube-wave amplitudes well correspond to those of the multiple open fractures. Furthermore, the effect of large dip angles is extensively discussed. The approximate solution (the Mathieu functions) and the numerical modeling results (FEM) reveal that the effect of the dip angle is significant for a thick structure and large dip angles. The developed theory is important to evaluate field data which contain the effects of tube waves due to dipping, permeable layers, e.g., cataclasite layers and fault gouges.

Introduction

Subsurface fractures play an important role in determining fluid flow and deformation process in rocks. Therefore, characterizing their hydraulic properties is significant in oil/gas exploration and in seismology. In VSP experiments using a fluid-filled borehole, it is well known that low-frequency Stoneley waves (tube waves) are generated at fractures intersecting the borehole (e.g., Beydoun et al., 1985). This is caused by fluid exchange between the borehole and the fracture due to the deformation of the fracture by an incident P wave, which gives a direct measure of the hydraulic properties of the fracture. The tube waves have extensively been studied in the past in order to characterize fractures intersecting a borehole (e.g., Beydoun et al., 1985; Hornby et al., 1989).

Conventionally, the models of tube-wave generation have considered the fluid flow due to the deformation of (1) a parallel-wall open fracture (Beydoun et al., 1985; Hardin et al., 1987; Ionov, 2007; Bakku et al., 2013) or (2) a permeable layer (Li et al., 1994). The former is found to be useful to estimate the permeability corresponding to μm-to-mm scale fractures (e.g., Hardin et al., 1987; Hornby et al., 1989), whereas the latter is useful for larger-scale (cm-to-m) geological faults (e.g., Li et al., 1994; Kiguchi et al., 2001).

There are wide varieties of theories for the parallel-wall open fracture model. Beydoun et al. (1985) first considered the tube-wave generation using the Darcy's law (low-frequency approximation). They assume that the deformation of the fracture aperture is equivalent to the displacement amplitude of the incident P wave and it is uniform everywhere along the fracture. Furthermore, they assume that the fluid pressure perturbation at the fracture-borehole intersection is negligibly small (Beydoun's boundary condition), which is valid for small-amplitude tube waves. Hardin et al. (1987) extended Beydoun's approach by considering that the incident stress is uniform everywhere along the fracture so that they can correctly include the stiffness of the fracture in the deformation process. Ionov (2007) removed the small-amplitude assumption of the Beydoun's approach by considering a realistic boundary condition that the fluid pressure at the fracture-borehole intersection is equivalent to the tube-wave generation amplitude (Ionov's boundary condition). Bakku et al. (2013) further extended the Ionov's approach by considering the dynamic flow condition so that the theory is available for a wide range of frequencies.

Contrary to the parallel-wall open fracture model, there is only one theory available for the permeable-layer model (Li et al., 1994). This model considers that the deformation of the layer is uniform everywhere and uses the Beydoun's boundary condition. This implies that the theory does not correctly account for the stiffness of the layer on the deformation process, and the theory is not valid when the amplitude of tube wave is large. Furthermore, natural fractures are often not horizontal. All the theories so far consider the cylindrical coordinate system, i.e., horizontal structures. A few studies consider a modification of the horizontal structure model due to the small dip angles (Beydoun et al., 1985; Li et al., 1994). The tube-wave reflection and transmission problem in acoustic logging (e.g., Hornby et al., 1989; Tang and Cheng, 1993) propose approximate solutions for dipping structures. However, they are not appropriate when (1) the dip angle is high and/or (2) the thickness of the dipping structure is larger than the diameter of the borehole. This is extremely problematic for field tube-wave data from cataclasite layers and/or fault gouges at a fault-damaged zone (e.g., Kiguchi et al., 2001).

In this study, we develop a new theory for tube-wave generation due to a permeable layer. This is a major extension of the conventional permeable-layer model: the new model correctly accounts for the stiffness of the layer in the deformation process and it is also valid for large-amplitude tube waves. Furthermore, we use numerical modeling (finite element method) in order to correctly consider the effect of the dip angles. As a comparison, we also derive the approximate solution of the dipping structure using the Mathieu functions. The developed theory will be essential for tube-wave generation analysis for permeable layers with large dip angles, such as, cataclasites and fault gouges at fault-damaged zones.

Theory of tube-wave generation

We consider that a permeable layer is deformed due to the incident stress field which causes fluid flow and generates tube waves (Figure 1a). Similar to the open fracture model (Hardin et al., 1987; Bakku et al., 2013), we assume that the dynamic layer thickness $L(t)$ is determined from the layer compliance Z_L (m/Pa) and the effective stress in the layer as $L(t) = L_0 + Z_L(p(t) - \sigma_n(t))$, where L_0 is the static thickness, p the fluid pressure perturbation, and σ_n the incident stress field acting normal to the layer. Here we assume that the stress field is uniform everywhere along the layer (Hardin et al., 1987), which is the main difference from the foregoing study (Li et al., 1994). It enables us to obtain the explicit connections between the permeable layer model and the open fracture model, which is discussed in a later section. Considering the quasi-static approximation (Nagy, 1992), the layer compliance can be represented as $Z_L \approx L_0/\rho V_P^2$.

Similar to the foregoing studies (e.g., Li et al., 1994; Bakku et al., 2013), the equation of continuity for the fluid flow due to the deformation of the layer is considered. This results in a partial differential equation for the fluid pressure perturbation in the layer as,

$$\nabla^2 \hat{p} + \xi^2 \hat{p} = A, \quad \text{where} \quad \xi^2 = -i\omega \frac{\mu\phi}{\kappa_0}\left\{K_f^{-1} + \frac{Z_L}{L_0}\right\} \quad \text{and} \quad A = i\omega\sigma_0 \frac{Z_L \mu \phi}{L_0 \kappa_0}, \tag{1}$$

where $\hat{p}$ is the fluid pressure in the frequency domain, σ_0 is the amplitude of incident stress field, μ the fluid viscosity, K_f the fluid bulk modulus, ϕ the porosity of the layer, and κ_0 the static permeability. Here we linearized the equation by neglecting the higher-order terms (Bakku et al., 2013). Equation (2) is valid for dipping structures as well as for horizontal structures. For a cylindrical coordinate (i.e., a horizontal structure), we replace ∇^2 as $\partial/\partial r^2 + r^{-1}\partial/\partial r$, where r is the radial direction.

The tube-wave generation amplitude (p_t) is determined from the fluid flow rate incoming to the borehole Q_g (m^3/s) as (Ionov, 2007),

$$p_t = \frac{\rho_f c_T}{2\pi R} Q_g, \quad \text{where} \quad Q_g = -\frac{L_0 \kappa_0}{\mu} \int_S \nabla \hat{p} d\mathbf{S}, \tag{2}$$

where ρ_f is the fluid density, c_T the tube-wave velocity, R the borehole radius, and $\mathbf{S}$ indicates surface area of the fracture-borehole intersection. Note that the fluid flow rate (Q_g) is determined from the fluid velocity at the fracture-borehole intersection and we use the Darcy's law. The pressure distribution (p) is obtained from the partial differential equation (Equation 2) considering the boundary conditions at the fracture-borehole intersection. The two different boundary conditions have been proposed: (1) Beydoun's boundary condition ($\hat{p} = 0$) and (2) Ionov's boundary condition ($\hat{p} = p_t$). The former is the approximation of the latter and it is valid when the pressure at the intersection is negligibly small. For a cylindrical coordinate (a horizontal structure), the boundary condition is evaluated at $r = R$, and we obtain the analytical solution of $\hat{p}(r)$ using the modified Bessel function K_0:

$$\hat{p}(r) = BK_0(\xi r) - \xi^{-2}A, \quad \text{where} \quad B = \begin{cases} \xi^{-2}AK_0^{-1}(\xi R) & \text{Beydoun's B.C.} \\ (p_t + \xi^{-2}A)K_0^{-1}(\xi R) & \text{Ionov's B.C.} \end{cases}. \tag{3}$$

After obtaining the tube-wave amplitude, we evaluate the tube to P-wave amplitude ratio ($\gamma_g = p_t/p_i$), where p_i is the incident amplitude observed in the borehole (e.g., Bakku et al., 2013).

Efficacy of the new model

Here we check the efficacy of the developed permeable-layer model by making an explicit connection with the parallel-wall open fracture model developed by Bakku et al. (2013). To this end, we assume that the permeable layer is represented by multiple fractures with same apertures L_0^{OF} (Figure 1b). The effective tube-wave generation amplitude due to the multiple fractures can be calculated using the representation theorem (Minato et al., 2016). When we specify the layer thickness (L_0), porosity (ϕ) and permeability (κ_0), then we obtain the corresponding number of the open fractures (N) and fracture aperture (L_0^{OF}), which gives the equivalent permeability (Tang and Cheng, 1993).

We consider horizontal structures with normally incident P wave, and calculate the tube to P-wave amplitude ratio (γ_g). Figure 1c indicates the comparison between the new permeable-layer model ($L_0 = 0.2$ m, $\phi = 30$ %, $\kappa_0 = 10$ Darcy, $V_P = 3500$ m/s, $V_S = 2000$ m/s, $\rho = 2500$ kg/m^3) and the effective tube-wave generation amplitude due to multiple open fractures ($N = 3020$, $L_0^{OF} = 19.9$ μm). One can see that the permeable layer model is very well represented by multiple open fractures, especially at low frequencies. The discrepancy at high frequencies is due to the effect of the dynamic fluid flow condition in the open-fracture model (Bakku et al., 2013), which is not considered in our theory (i.e., Darcy's law or low-frequency approximation).

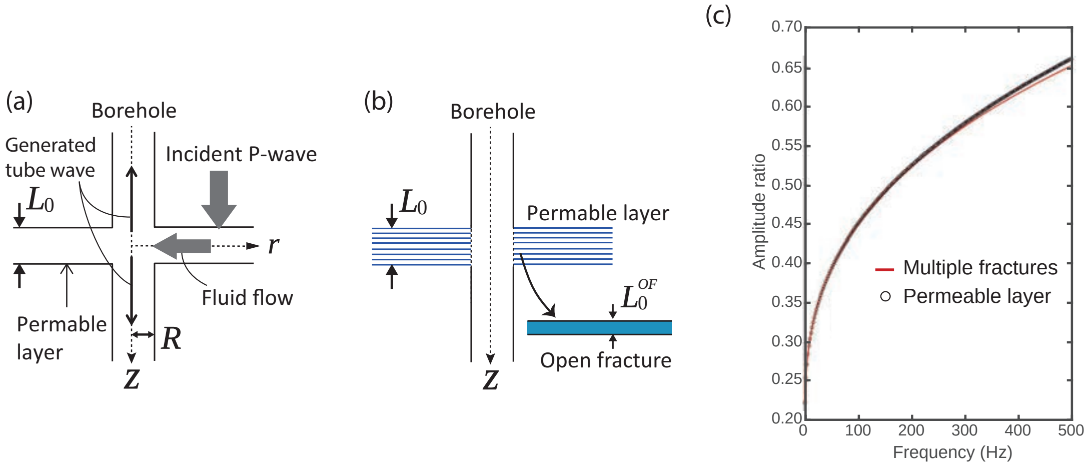

***Figure 1** (a) Configuration of tube-wave generation due to a permeable layer. (b) Permeable layer represented by multiple open fractures. (c) Tube to P-wave amplitude ratio for the new permeable layer model and the multiple fractures.*

Effect of dip angles

When the dipping structure is intersecting the borehole, the boundary of the fracture-borehole intersection becomes dipping elliptic cylinder (Figure 2a). The semi-major and semi-minor axes of the ellipse depend on the dip angle θ (Tang and Cheng, 1993). The approximate analytical solution is available when this boundary is replaced by the vertical elliptic cylinder (red lines in Figure 2a), which reduces Equation (2) into an elliptical coordinate system. The solution contains the Mathieu functions (e.g., Hornby et al., 1989) instead of the Bessel function. As an alternative, we can evaluate the boundary condition at the dipping elliptic cylinder by numerically solving Equation (2). For this purpose, we use finite element method (FEM).

Figure 2b is the pressure distribution obtained using FEM when the dip angle is 40° (other parameters are equivalent to those in the previous section). For brevity, we use the Beydoun's boundary condition (see the previous section). After obtaining the pressure field, we calculate the tube to P-wave amplitude ratio (γ_g) with normally incident P wave for $L_0 = 0.2$ m and $L_0 = 0.02$ m (Figure 2c and 2d), respectively. Here we consider various dip angles. The continuous lines in Figure 2c and 2d indicate the analytical solutions using the Mathieu functions with the assumption of the vertical elliptical cylinder boundary (red lines in Figure 2a). One can see that this approximate solution is valid for small dip angles with small thickness (Figure 2d). For a thick structure, the deviation between the FEM results and the approximate solution is quite large (Figure 2c), suggesting that the effect of the dip angle is significant and the numerical modeling approach is required in order to correctly evaluate the tube-wave generation amplitude.

Conclusions

We derive a new theory for tube-wave generation due to a permeable layer. The new model is very well represented/explained by the multiple open fracture model which was developed earlier. Showing the connection between the open fracture model and the permeable layer model was not possible so far. We also show a numerical modeling approach to correctly account for the effect of the dip angles. A

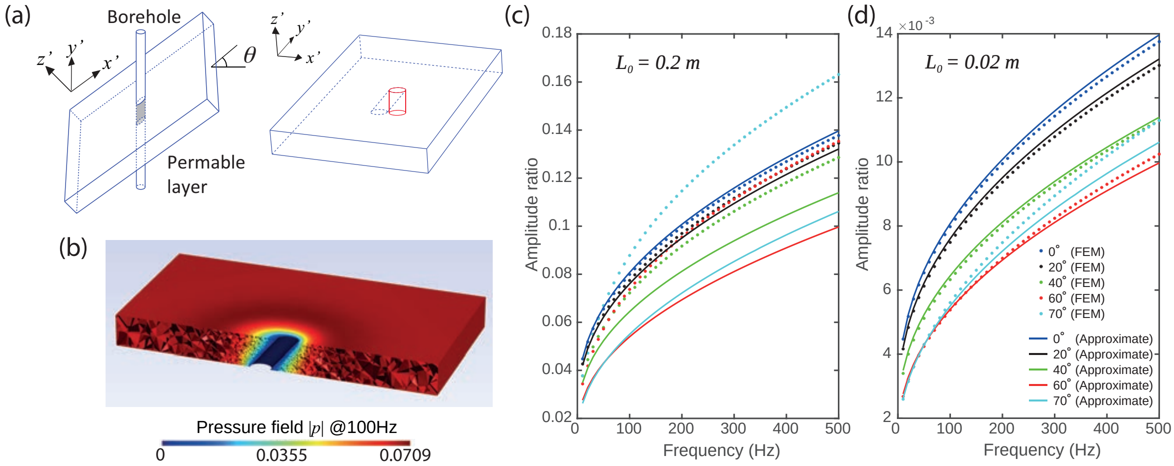

Figure 2 *(a) Configuration of the dipping structure and the elliptical cylinder boundary at the fracture-borehole intersection. The red vertical elliptical cylinder is assumed for the approximate solutions. (b) Pressure distribution using FEM with exact elliptical cylinder boundary. (c) Tube to P-wave amplitude ratio from the FEM and the approximate solutions assuming the vertical elliptical cylinder boundary. (d) Same as (c) but for a thin structure (L_0 =0.02 m).*

comparison between the approximate analytical solution using the Mathieu functions and the results of FEM reveals that the effect of the dip angle is significant for a thick structure and large dip angles. The developed method can be advantageously be used to field data where the effect of cataclasites or fault gouges with large dip angles is dominant, e.g., the estimation of permeability structure in fault-damaged zones.

Acknowledgements

This work is supported by The Netherlands Research Centre for Integrated Solid Earth Science.

References

Bakku, S.K., Fehler, M. and Burns, D. [2013] Fracture compliance estimation using borehole tube waves. *Geophysics*, **78**(4), D249–D260.

Beydoun, W., Cheng, C. and Toksöz, M. [1985] Detection of open fractures with vertical seismic profiling. *Journal of Geophysical Research: Solid Earth (1978–2012)*, **90**(B6), 4557–4566.

Hardin, E., Cheng, C., Paillet, F. and Mendelson, J. [1987] Fracture characterization by means of attenuation and generation of tube waves in fractured crystalline rock at Mirror Lake, New Hampshire. *Journal of Geophysical Research: Solid Earth (1978–2012)*, **92**(B8), 7989–8006.

Hornby, B., Johnson, D., Winkler, K. and Plumb, R. [1989] Fracture evaluation using reflected Stoneley-wave arrivals. *Geophysics*, **54**(10), 1274–1288.

Ionov, A.M. [2007] Stoneley wave generation by an incident P-wave propagating in the surrounding formation across a horizontal fluid-filled fracture. *Geophysical prospecting*, **55**(1), 71–82.

Kiguchi, T., Ito, H., Kuwahara, Y. and Miyazaki, T. [2001] Estimating the permeability of the Nojima Fault Zone by a hydrophone vertical seismic profiling experiment. *Island Arc*, **10**(3-4), 348–356.

Li, Y., Rabbel, W. and Wang, R. [1994] Investigation of permeable fracture zones by tube-wave analysis. *Geophysical Journal International*, **116**(3), 739–753.

Minato, S., Ghose, R., Tsuji, T., Ikeda, M. and Onishi, K. [2016] Modeling and imaging of multiply generated and scattered tube waves due to multiple hydraulic fractures. *SEG Technical Program Expanded Abstracts 2016*, 682–687.

Nagy, P. [1992] Ultrasonic classification of imperfect interfaces. *Journal of Nondestructive Evaluation*, **11**(3-4), 127–139.

Tang, X.M. and Cheng, C. [1993] Borehole stoneley wave propagation across permeable structures. *Geophysical prospecting*, **41**(2), 165–187.